ICAS 2021 SHANGHAI
International Council of the Aeronautical Sciences
32nd Congress of the International Council of the Aeronautical Sciences
September 6-10, 2021
Pudong Shangri-La, Shanghai, China

AIRLINE NETWORK-AIRPLANE INTEGRATED OPTIMIZATION CONSIDERING MANUFACTURER'S PROGRAM COST

José Alexandre T. G. Fregnani Bento Silva de Mattos & José Antonio Hernandes

Instituto Tecnológico de Aeronáutica (ITA)
12228-900 São José dos Campos, São Paulo, Brazil

Abstract

Aerial network routes and their flight frequencies are crucial for the strategic planning of airlines. Airlines must choose optimum airplane types to improve revenue and to reduce operating costs. In addition, aircraft manufacturers need to identify airplane configurations that better suit airline operations and establish list prices for their products as well as calculate the production and development costs of their products. To address these issues, the present study describes and applies a methodology to determine the optimal aerial transport network simultaneously with the identification of the optimum fleet for that network, namely, an integrated design. In the optimization simulations carried out in the present work, the objectives are the maximization of the operational cost of the airline and the minimization of the airplane fleet cost. Each fleet is composed of three types of airliners, selected according to their passenger capacity. Airplanes are designed with high-fidelity methods, realistic performance calculations and must obey a set of requirements, including some related to FAR 25 certification rules. Optimization for a Brazilian network considering 21 cities was carried out with the maximization of the network's daily profit and the minimization of the fleet acquisition cost. A comprehensive airplane manufacturer program cost estimation model was implemented, enabling the calculation of the net present value of a transport airplane program and financial parameters.

Keywords: aircraft design; multi-disciplinary design and optimization; airline network

1. Introduction

The steady need for reduction of operational cost is widely agreed on by the civil aviation industry, which is known to present low-profit margins, with the average world airline margins ranging from -4 to 3% [1]. Thus, there is room to improve the operations to assure survivability in a harsh competitive environment. Optimization techniques are a suitable tool to deliver improved airline operation possibilities.

Optimization methods have been widely applied to reduce operational costs, such as fuel-efficient flight paths, optimum slot allocation, and turnaround time reduction [2] [3] [4] [5]. They are applied to the operational planning process of airlines, which is divided into three major blocks, as shown in Figure 1. Due to the interdependence of the blocks shown in Figure 1, optimization models are usually set up to solve the entire cycle problem, considering minimization of costs or maximization of revenues as objective functions in a multi-objective optimization problem [3]. However, with this approach, large-scale problems may arise, with the utilization of non-linear programming algorithms and therefore large computational power may be required to get the problem solved. The most common solution adopted is the optimization of each block separately.

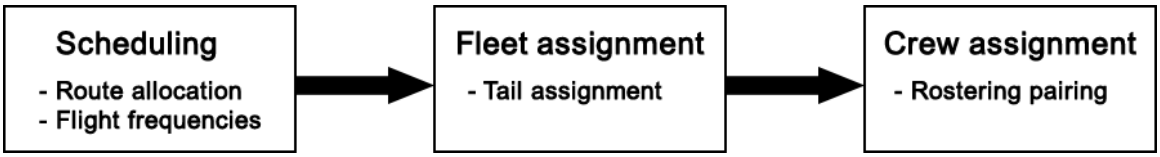

Figure 1 - Typical operational planning process of airlines.

The selection of the aircraft fleet types suited for the network is indeed performed before the optimization of the first block, which is a significant factor that influences the flight frequencies. The determination of the optimal flight network and associated frequencies is a key step for airlines to elaborate their strategic planning, from market determination to aircraft and crew rostering. An optimal solution for this block facilitates the solution for the others. Furthermore, if the optimum aircraft types are associated with the assigned network, revenue and/or minimum operational costs can be improved even further. In other words, network optimization is normally carried out separately from aircraft optimization in the airline planning process.

Due to its complexity, the aircraft design process is divided into phases: feasibility study, conceptual design, preliminary design, and detailed design [6]. The conceptual design phase identifies the various conditions of the mission and synthesizes a set of initial aircraft configurations capable of performing the mission. For commercial aircraft, the mission is defined by airline requirements, which typically include direct operating cost for some few routes, payload requirements, range along a proposed service route, traffic volume and frequency, and airport compatibility; the latter usually translated into field performance, ground maneuvering, and terminal service. Several configurations are evaluated in the conceptual phase and aircraft manufacturers may decide to further investigate one or more concepts that fulfill all requirements [7]. Typically, the development phase of a civil aircraft lasts five years and the conceptual phase takes one year to select one or more configurations. The recurrent and non-recurrent costs of an aircraft project are internally modeled here based on the formulation of Mattos et al. [6]. For this, it is necessary to estimate the aircraft list price, which is obtained from a market outlook methodology [8]. The purchase price for the airline's optimal fleet is one of the objective functions of the present work.

Complex aerial networks are used here to conceptually design airliners within an integrated design. There are already studies in this context, but most of the aircraft models are very simple [9]. Aircraft manufacturer designs are focused mostly on subsystem requirements, usually ignoring the high degree of dependency that exists between airplanes and networks. There is a need for an integrated design process, where both aircraft - or a family of aircraft - and aerial networks are optimized simultaneously [6] [10]. On the airplane part of this problem, this task is carried out in the conceptual phase.

The optimization framework of the present work embraces the determination of the optimal aerial transport network simultaneously with the optimum aircraft fleet for this network. The fleet can be composed of an arbitrary number of jet airplane types or versions. Airplanes were selected for an optimization task according to passenger capacity: 44 to 69 for the first model; 70-99 for the second; and 100-156 for the third. Aircraft design is integrated into any airline network of interest, considering a realistic operational profile, comprising airport runway information, course, and passenger demand raised by a gravitational model. The determination of the optimum network considers a two-stop route model and three jet airplane types composing the fleet. Optimal airplane fleets are obtained considering maximization of net profit and manufacturer aircraft fleet list price. A Mixed-Integer Linear Programming (MILP) algorithm [11] obtains the network with maximum operational profit.

A database of airplanes with the most distinguished characteristics is employed in the optimization process. The optimal fleet is then determined from the combination of airplanes that compose that database. Besides the faster convergence of optimization processes, optimal airplanes can be further improved in an off-design approach and their impact on the network can be easily analyzed. Many design parameters are used to represent the airplane in the finest detail with accurate aerodynamic, structural analysis, stability and control, and performance calculations.

In the present work, airplanes are generated according to the following design features:

a. Adherence to Federal Aviation Regulations FAR 25 requirements and others like balanced takeoff field length, landing field length, range with given payload, stall location outside the aileron region, and enough fuel storage to comply with certain missions.
b. Calculation of noise signatures at International Civil Aviation Organization (ICAO) certification points: sideline, approach, and takeoff [6]. Engine emissions [6] are also calculated for any airplane and can be considered in the optimization process if requested.
c. A new own method for turbofan engine weight estimation [10]. Flaps are designed not to be affected engine hot exhaust gases. The wheels of the main landing gear are accommodated inside the wing-fuselage fairing. Engines of underwing configurations are positioned to avoid uncontained fan debris hitting fuel tanks. Wheel tires are selected from tables containing internal pressure, loads, speed, and other parameters. The main landing gear trunnion is positioned between the rear and auxiliary spars of the inner wing. Ditching and cargo requirements are considered for fuselage cross-section sizing.
d. An Artificial Neural Network (ANN) system is used to calculate the aerodynamic characteristics of the airplane configurations [12]. Stability derivatives are calculated with the AVL vortex-lattice code [13] and the methodologies to design the horizontal and vertical tails are described by Secco and Mattos [14].

The optimization framework described in the preceding paragraphs enables:

- Aircraft manufacturers to fully integrate their concepts with airline operations. Over sixty airplane design variables assure a detailed conceptual design for airplanes.
- Aircraft to evaluate the operational characteristics of a competitor airplane in a network of airlines interested to place an aircraft order.
- Airlines to find out the optimal fleet jointly with the optimal network for their operations.
- An airline to estimate its operational cost and profit with a combination of jet airplanes on its fleet.
- Airlines can estimate aircraft emissions (NOx and CO2) of their daily operations more accurately. The same is true for aircraft manufacturers.
- Evaluate the impact of the incorporation of a new jet aircraft type or a version of an existing one on its profit and cost structure.

2. Methodology

2.1 Overview of the optimization framework

The Multi-disciplinary Design and Optimization (MDO) framework is shown in Figure 2 where, as exemplification, the optimal aircraft fleets, are composed of three aircraft types. Objectives are the maximization of network profit (NP), satisfying given city-pair passenger demands, and the minimization of fleet acquisition list price. MATLAB® is employed as an integrating platform. The airplane databases (DB) were built according to three ranges of passenger capacity. The first one considers 13 airplanes with capacity ranging from 44 to 69 seats; database No. 2 hosts 12 airplanes transporting between 70 and 99 passengers; finally, the third database has 17 types of

airplanes featuring between 100 and 156 seats. Thus, there are 2,652 potential combinations to be explored in the design space. A routine retrieves all the necessary data related to the three selected airplanes such as engine parameters, weights, fuel capacity, noise signature, passenger accommodation, fuselage dimensions, range, and others. The Mission performance module calculates the fuel burn, trip time, and Direct Operating Cost (DOC) for a mission between the departure and destination airports. Moreover, it also provides takeoff weight and ambient conditions. This module calls the aerodynamic and propulsion module routines to determine the necessary fuel flow and drag for the trajectory calculations.

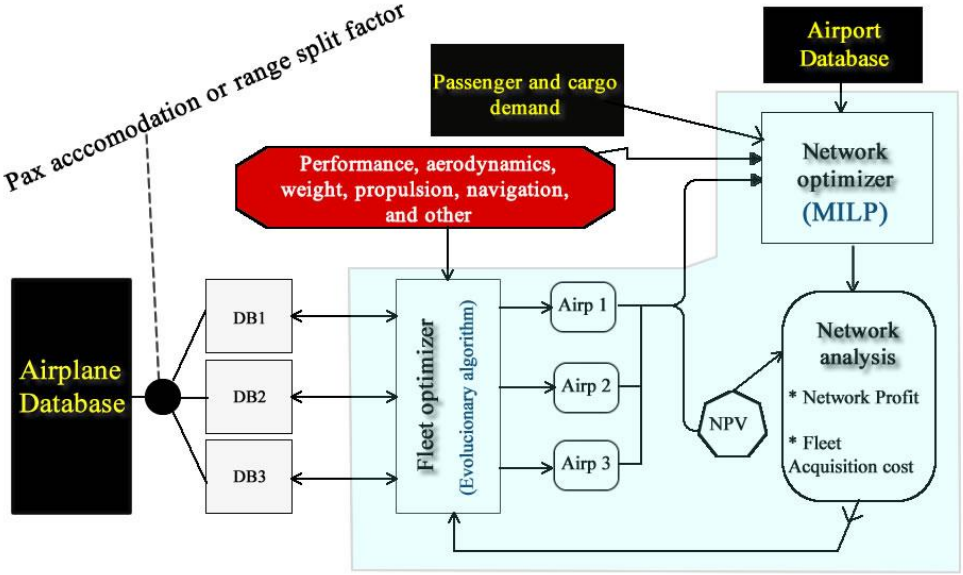

Figure 2 - Airplane/Network integrated design optimization framework.

The network optimizer module embodies a Mixed Integer Linear Programming problem. MILP problems are generally solved using a linear-programming-based branch-and-bound algorithm [11] [15]. Typically, the LP-based branch-and-bound procedure begins with the original Mixed Integer Programming (MIP). Moreover, not knowing how to solve this problem directly, all the integrality restrictions are removed. The resulting Linear Programming (LP) is called the linear-programming relaxation of the original MIP. It is then possible to solve this LP. It is a matter of chance if the result happens to satisfy all the integrality restrictions, even though these were not explicitly imposed. This solution is an optimal solution of the original MIP, and the search for the optimal solution is over. If not, as usually the case, the normal procedure then is to pick a variable that is restricted to be an integer, but whose value in the LP relaxation is fractional. To obtain an upper bound on the objective function, the branch-and-bound procedure must find feasible points. A solution to an LP relaxation during branch-and-bound can be integer feasible, which can provide an improved upper bound to the original MILP. Certain techniques find feasible points faster before or during branch-and-bound. Most MILP algorithms, including the one used here, use these techniques at the root node and during some branch-and-bound iterations. These techniques are heuristic [11], meaning they are algorithms that can both succeed and fail. The optimum networks for a set of three airplane types are determined simultaneously based on airport and econometric information, retrieved from a database, aircraft maximum passenger capacity, aircraft design range, and associated DOC. This is an optimization task within another on a higher level (Figure 2).

In the Network analysis module, fuel burn, trip time, and DOC for all sectors are calculated and compiled to calculate the total profit of the network operation and Manufacturer´s Cashflow Net Present Value; the latter delivering as a by-product the list price of all airplanes from the database. The fleet Optimizer module generates the design variables, the set {Airp 1, Airp 2, Airp 3}. These are indeed integer variables directly linked to database indexes of the airplanes. After this, all data related to the airplanes are passed to the performance module. Network profit and the fleet acquisition price are processed in this module. The Multi-objective genetic algorithm MOGA-II [16] was employed in the computations carried out here. It is robust and can handle global minima or maxima inside a complex design space built with many variables. The optimization generations were made of 20 individuals. Design ranges for the airplanes of the three databases are defined at the point of typical single-class passenger capacity considering takeoff with maximum takeoff weight (MTOW). Each aircraft in the databases is represented by 61 parameters, which are associated with their airframe, performance, propulsion, and aircraft systems. Some constraints and certification requirements are presented in **Tables I** and **II**.

The aircraft database is generated through random variation of most parameters within a specific interval, as listed in Tables I and II. Some parameters of tail surfaces are kept constant in this study to simplify the tail sizing computations. For the airplane design, Maximum Takeoff Weight, Maximum Landing Weight, and Operational Empty Weight of each aircraft are calculated through an iterative process which is illustrated in Figure 3. In this calculation, the weight of engine nacelles, fuselage, empennage, airplane systems, landing gear are calculated separately using empirical formulae [17] [18]. The wing weight is calculated by sizing the wingbox to withstand aerodynamic loads calculated with a full potential code in a few maneuvers in the flight envelope [19]; moreover, the weight of the secondary wing structure is estimated by empirical methods. All these weights are considered for the determination of the operating empty weight. With the weight of each component, it is also possible to obtain the center of gravity of the aircraft and its variation with fuel consumption and different payloads [17]. MTOW and maximum landing weight (MLW) are then estimated interactively using the mission analysis module and the calculated operating empty weight (OEW) of the given design range [10]. The AVL code [13] is employed for the calculation of stability derivatives for tail sizing.

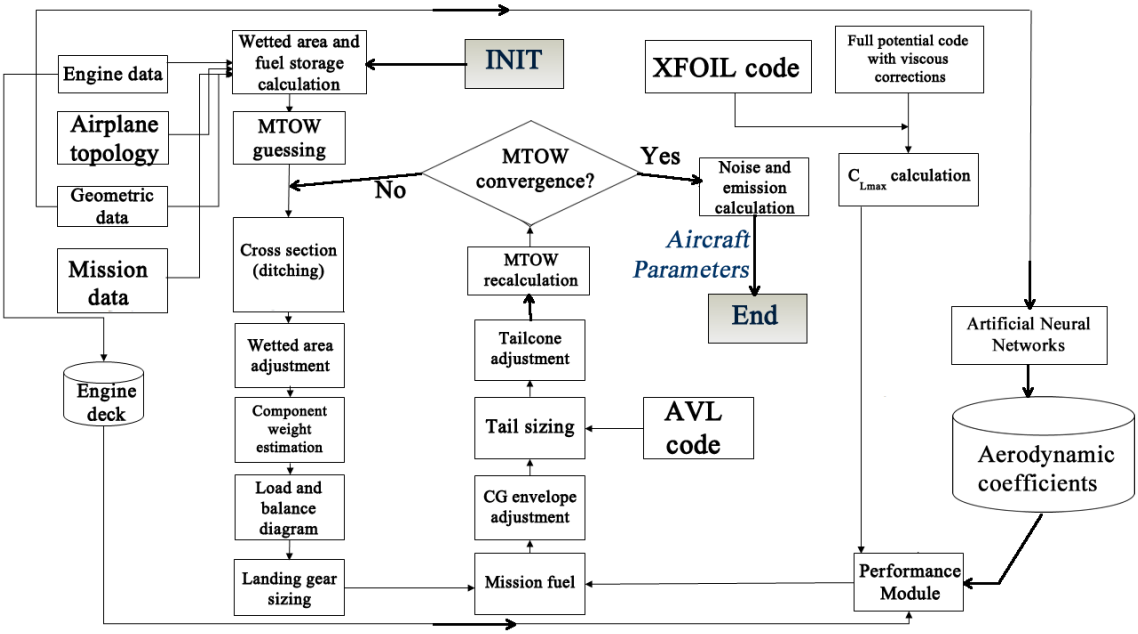

Figure 3 - Flowchart of airplane calculation including key airplane weights.

Table I - Airframe and performance parameters

Parameter	Characteristic/Value
Passenger cabin external width	Calculated to fulfill clearances, ditching, container type, and other cabin parameters or requirements
Passenger cabin external height	Calculated to fulfill clearances, ditching, container type, and other cabin parameters or requirements
Fuselage length	Based on seat arrangement, emergency exits, galley, and toilet areas
Tailcone	Adjusted to host tailplanes, engine (if placed there), and some aircraft systems like the auxiliary power unit (APU)
Passengers at 32-in pitch	From 44 to 156 (single class)
Number of aisles	1
Seating abreast	4 - 6
Cabin crew	1 + 1 for every 50 passengers
Cabin aisle width [m]	0.50 m (It may suffer changes to comply with ditching requirements)
Cabin height [m]	2.00 m
Seat width [m]	0.46 m
Container type	None or LD-45W
Horizontal tail (HT) configuration	Conventional or “T” tail
Wing airfoil	Each basic airfoil used in the wing is defined by 14 parameters
Wing reference area [m^2]	48 ➔ 124
Wing aspect ratio	7.5 ➔ 9.2
Wing taper ratio	0.25 ➔ 0.43
Wing sweepback angle at quarter chord	20^o ➔ 28^o
Flap deflection @ takeoff	35^o
Flap deflection @ landing	45^o
Slat	Can optionally be incorporated into the configuration with a weight penalty and improved C_{Lmax}
Location of break station (fraction of semispan)	0.31 ➔ 0.34
Incidence angle at the wing root	2 ➔3^o
Incidence angle at break station	0 ➔ 0.5^o
Incidence angle at the wingtip	-1 ➔ -5^o
Winglet	Can be considered or not into the configuration
Service ceiling [ft]	37,000 - 41,000
Range with typical payload [nm]	1,290 - 2,400 (MTOW, takeoff from sea level, ISA)

Table II - Power plant Parameters

Parameters	Min - Max
Engine diameter D_e [m]	1.14 - 1.52
By-pass ratio (BPR)	3.04 - 6.20
Fan pressure ratio	1.32 - 1.85
Overall pressure ratio	21.00 - 30.00
Turbine inlet temperature [K]	1320 - 1420
Number of jet engines	2
Engine location	Underwing configuration or at the rear fuselage

2.2 Network Optimizer

Provided the airplane triplet {Airp 1, Airp 2, Airp 3} is known, the optimum network, including the necessary frequencies, is solved in a secondary optimization process using a mixed linear programming algorithm. Allocation tail assignment and schedule for each frequency are not considered in the present framework. The airline networks are optimized considering operations within a certain geographical area with a certain market share. For this, passenger demand among airports, average ticket price, aircraft fleet capacity, range, and operational costs must be known. Then, an optimized network can be drawn up considering the profit maximization. In this context, the profit is maximum if all potential passenger demand is fulfilled for each city pair, allocating the necessary frequencies for each aircraft type. Also, it is assumed that the airline allows passengers to buy tickets for a maximum of two stops between origin and destination, meaning that three types of services are possible: non-stop flights, one-stop connecting flights, and two-stop connecting flights. This is a common policy practiced by Brazilian domestic airlines nowadays.

The linear programming optimization algorithm in this module was based on that elaborated by Jaillet, Song, and Yu [20] for generic network determination considering passenger's fractional flow. The mathematical formulation of the problem is presented in the next paragraphs.

Let X_{iltj} be the fraction of the passenger's demand flow f_{ij} from the origin, *i* to destination *j*, served by a two-stop connecting flight through cities *l* and *t*, Y_{ijk} the number of aircraft type k used in the route from city *i* to *j*, *p* the average fare per passenger (US$), c_k the average operational cost ($/nm) at design range, b_k is the passenger capacity of aircraft *k*, the reference load factor LF_{ref} and d_{ij} the distance between origin and destination airports. The following integer linear programming model is proposed:

$$\text{Maximize} \quad \sum_{i \neq j} \sum_{k} k_1.p - k_2.\frac{(c_k.d_{ij})}{LFref * b_k} \tag{1}$$

subject to:

$$f_{ij} + \sum_{t \neq i,j} \left(f_{it}.X_{ijt} + f_{tj}.X_{tij} - f_{ij}.X_{itj}\right) + \sum_{i,t \neq i,j} \left(f_{lj}.X_{ltij} + f_{it}.X_{ijlt} - f_{ij}.X_{iltj}\right) \leq \sum_{k} LFref, b_k.Y_{ijk} \quad \text{for all } i \neq j \tag{2}$$

$$\sum_{t \neq i,j} X_{itj} + \sum_{l,t \neq i,j} X_{iltj} \leq 1 \quad \text{for all } i \neq j \tag{3}$$

where X_{itj}, X_{iltj} are positive and Y_{ijk} integer positive for all $i \neq j$

The average operational costs (C_k) for each aircraft fleet, necessary for the optimization, correspond to DOC related to the design range mission. The objective function is set to maximize the network profit, based on the difference between the average fare and the average cost per passenger. A constraint states that the fractional flow on route *ij* cannot exceed the total capacity of the aircraft assigned, while another constraint ensures that the passenger flow from a direct flight from *i* to *j* is non-negative. It is assumed that 50% of all passenger demand from *i* to *j* are derived from direct flights (X_{ij} and X_{ji}), 30% distributed equally among all one-stop flights (X_{ijt}, X_{tij} and X_{itj}) and 20% distributed equally among two-stop flights (X_{ltij}, X_{ijlt} and X_{iltj}). Passenger potential demand between origin and destination (f_{ij}) is determined via gravitational model, based on city pair distance and econometric parameters. Let *P* be the city pair population product ($P=P_i.P_j$), *C* the city pair airport catchment area product ($C = C_i.C_j$), B the city pair combined Buying Power Index ($B = B_i + B_j$), *G* the city pair Gross Domestic Product (GDP) product ($G=GDP_i..GDP_j$) and d_{ij} the reference distance of the city pair.

The following passenger demand model is proposed:

$$f_{ij} = K_0 . P^{K1} . C^{K2} . B^{K3} . G^{K4} . {d_{ij}}^{K5} \quad (4)$$

In **Eq. 4**, the exponents K_0, K_1, K_2, K_3, K_4, and K_5 are calibration constants, determined by log-linear regression [21]. They may be easily calculated using the public econometric data available (P_i, C_i, B_i, and GDP_i often published by economic agencies).

2.3 Mission Analysis

In this module, the key results related to all air transport networks and all fleets of airplanes are aggregated. The computations of total profit of the network and total network operating cost (*NDOC*) are done via **Eq. 5** and **Eq. 6,** as a function of route frequencies ($Yijk$), departure and arrival delays ($DD_i \; and \; AD_j$), average delay cost per minute (*ID*), sector distance ($DIST_{ijk}$), aircraft passenger capacity (b_k) and average ticket price (p) as follows:

$$NDOC = \sum_{k=1}^{3} \sum_{i=1}^{N} \sum_{j=1}^{N} Y_{ijk} . (DOC_{ijk} + ID * (DD_i + AD_j)) \, , for \; i \neq j \quad (5)$$

$$NP = k_1 . \frac{p}{\sum_{k=1}^{3} \sum_{i=1}^{N} \sum_{j=1}^{N} d_{ijk}} - k_2 . \frac{NDOC}{\sum_{k=1}^{3} \sum_{i=1}^{N} \sum_{j=1}^{N} b_k . LF_{ref} . Y_{ijk}}, \qquad for \; i \neq j \quad (6)$$

In addition, the fleet size required in each aircraft type *k* may be estimated as a function of sector block time ($TB_{i,j}$) and average daily utilization (*DU*) according to:

$$TB_{ij} = T_{ij} + TIT + TOT + DD_i + DD_j \quad (7)$$

$$Nacft_k = int\left(\frac{\sum_{i=1}^{N} \sum_{j=1}^{N} TB_{i,j,k}}{DU} \right), for \; i \neq j \quad (8)$$

2.4 Propulsion and aerodynamics

Aerodynamics, performance, structural calculus, stability and control, and other major disciplines used for airplane build-up modeling are described by Fregnani, Mattos, and Hernandes [10]. However, due to the relevance and unique contribution of this research in the field of network optimization, some highlights of aerodynamics and propulsion models used here are described in this section.

Engine deck delivers fuel flow and net thrust necessary for performance and emissions calculations in all flight phases of the mission profile. The model utilized in the present work was implemented by Siqueira et al. [22]. The code is an improvement of the open-source code developed by NASA Glenn Research Center [23]. Improvements to this approach include compressor efficiency obtained by a complex interactive process from a basic compressor map. Besides flight condition, the set of input to the engine deck is composed of overall pressure ratio, engine fan pressure ratio, engine fan diameter, turbine inlet temperature, and throttle setting. Code output parameters are fuel flow, net thrust, mass flow, and exhaust Mach number among other important parameters that enable the calculation of engine noise (spectral frequency) and emissions.

Due to higher or even prohibitive computational costs arising from the utilization of higher fidelity tools, low-cost approximations of the physical systems are used instead of exact evaluations. In the context of optimization, surrogate models are typically used to approximate the objective function either globally or within a pre-specified trust region. Additionally, they can be employed to model a specific discipline like aerodynamics.

Aerodynamics provides valuable and critical information for other disciplines like performance, flight control, and load calculation. For this reason, the creation of accurate aerodynamic metamodels should contribute to speed up the design process. Multi-dimensional Interpolation (Look-up Table). Among several surrogate techniques, one of the most widely spread is the Kriging and co-Kriging or Gaussian process regression. According to prior attempts carried out by the authors, the use of Kriging techniques using freely distributed packages for the aerodynamic coefficient prediction of generic airplanes delivered unsatisfactory performance and showed a lack of accuracy. ANNs can deal both with many variables and nonlinear phenomena. The full potential code employed in the present work computes the viscous effects on the wing by interactively calling a boundary layer integral routine. The metamodel using ANNs is capable of accurately predicting the lift, drag, and pitching moment coefficients for any transport airplane with both arbitrary wing planform and airfoil geometry in subsonic and transonic flow regimes [12].

2.5 Aircraft list price

Besides the network operational profit, the aircraft fleet purchase amount is an objective function of the integrated design. To calculate the list price of the airplanes, it is necessary to proceed with a financial analysis of an aircraft project, comprising the phases of development and serial production. This analysis must consider the intended market share, aircraft list price, breakeven point, year of the return of investment, and internal rate of return (IRR), all key figures for an investment of a new or re-engined aircraft program [6]. In financial analysis, net present value refers to a series of cash flows over a given period. The present value of a cash flow (NPV), the time value of money, depends on the time interval between the beginning of accounting and the period of duration being considered, and on the interest rate. It provides a method for evaluating and comparing capital projects or financial products with cash flows spread over time, as in loans, investments, payouts from insurance contracts plus many other applications.

The following formula is used for NPV time calculation:

$$NPV(t) = \sum_{t=1}^{n} \frac{FC_t}{(1+r)^t} \begin{cases} t = time\ (years\ or\ months) \\ n = \ project\ time \\ r = \ minimum\ accepatble\ interest\ rate \\ FC_t = \ Net\ cash\ inflow - outflow\ at\ period\ t \end{cases} \tag{9}$$

The Net Present Value of the aircraft development and commercialization program is calculated from a set of inputs and hypotheses. This represents the sum of all *NPV(t)* along each year of the lifecycle of the project.

The cash flow is the difference between sales revenue and the development and production costs of the aircraft. In this study, the first 5 years of the product life are considered as the development phase, with no sales where non-recurrent costs are dominant, followed by 11 years as the production phase, where sales revenues and recurrent costs are dominant. It is also assumed that the minimum acceptable interest rate that may be interpreted as the minimum rate of which the capital could be potentially applied in another financial investment, is 5% per year. For the computation of the internal rate of return, the authors use the same formula as NPV. To derive the IRR, an analyst cannot rely on analytical methods. The higher a project's internal rate of return, the more desirable it is to undertake.

The following equation is then used for the IRR calculation:

$$0 = \sum_{t=1}^{n} \frac{FC_t}{(1 + IRR)^t} - Total\ initial\ Investment \tag{10}$$

IRR is uniform for investments of varying types and, as such, IRR can be used to rank multiple prospective projects on a relatively even basis. Assuming the costs of investment are equal among the various projects, the project with the highest IRR would probably be considered the best and be undertaken first. In the present work, the IRR is obtained with optimization by using the genetic algorithm to find out the market share that delivers the desired IRR. The project is considered feasible if IRR is at least 30%, representing the objective of an NPV optimization task. Thus, the aircraft program's financial structure is optimized to provide a desired internal rate of return. For this, the aircraft market share is the variable of optimization. The aircraft list price is dependent on the market share and a discount for a given percentage of the aircraft sold is considered, a common practice among manufacturers [24]. The methodology for the recurring and non-recurring cost calculation is strongly based on the one described by Mattos [6].

For the estimation of financial parameters of the aircraft program, it is necessary to estimate the revenue from aircraft sales. Therefore, the potential sales and sell prices must be known.

Camarotti elaborated a semi-automatic tool to issue market outlooks for commercial airplanes [8]. This tool gathers information and data such as oil prices and economic growth forecasts. Estimates of Revenue Passenger Kilometer are obtained from International Air Transport Association (IATA) annual reports. Air travel demand is derived from the match of two analysis methodologies: Bottom-up and top-down. The first one involves traffic forecasts within and between individual countries, based on economic estimates, growth momentum, historical series, attractiveness for travel, and liberalization and regulatory projections. Countries are then grouped by geographic regions for route identification within and between such regions. The top-down methodology projects the regional and global markets according to the aeronautical drivers and factors like technological, economical, policy, legislative, and other factors [8]. After the systemization of both methodologies, the specific characteristics of each region of the world are inserted in the model like population dynamics, the emergence of new means of transportation, and new secondary air services. Figure 4 shows some output graphs from Camarotti's tool for a 20-year-span market outlook starting in 2014. After the development and production cost structures alongside the size of the market for the airplane under analysis are established, the NPV and other parameters for the aircraft program can be calculated.

The design and production cycle parameters for Camarotti's program considered here are:

1. The period of the project of 16 years with 11 years of airplane serial production.
2. Internal rate of return of 30%.
3. Discount of 40% regarding the list price for 40% of airplanes to be sold.
4. List price depends on market share. An "S"-shape function was chosen to model this dependency.
5. Partners account for 30% of manufacturing. Partner labor cost is 50% higher than that of the manufacturer.

Figure 5 shows an example of cash flow and NPV for a 50-seater 16-year-long aircraft program. Figure 6 displays in a bar plot the production over years of the aircraft project under consideration. The NPV optimization task resulted in a market share of 46% of the total market demand for 2000 airplanes.

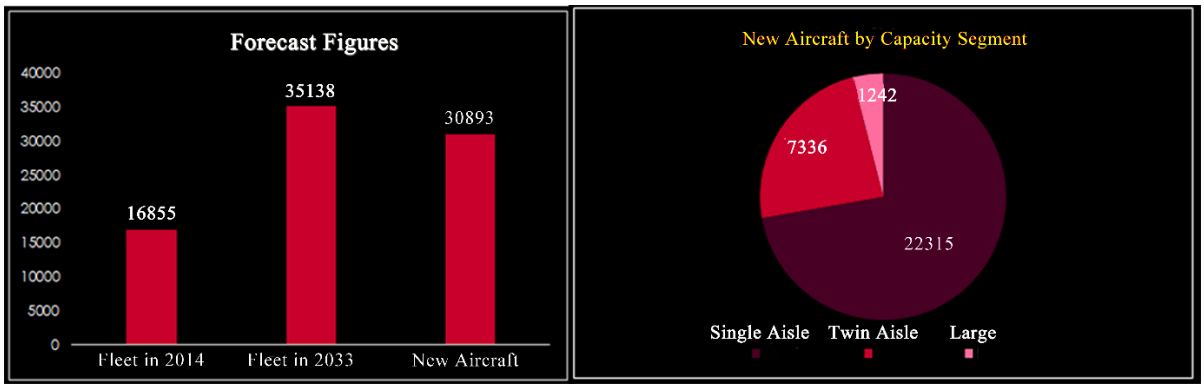

Figure 4 - Market outlook issued in 2013.

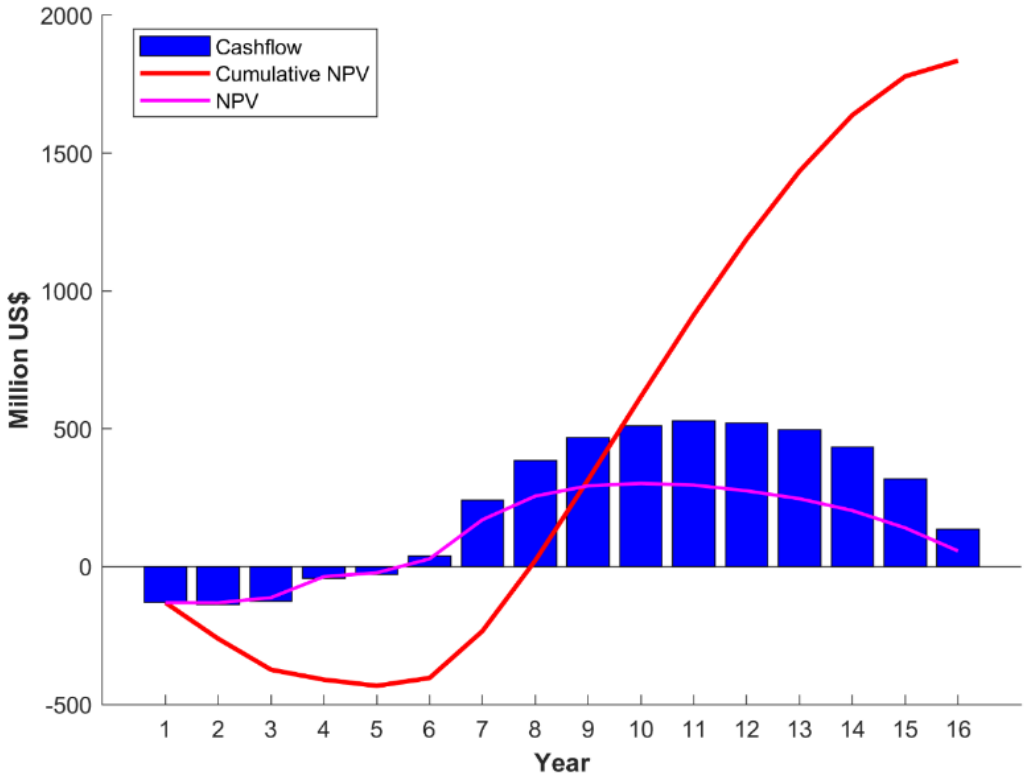

Figure 5 - Example of calculation of cash flow and cumulative NPV of a 50-seat airplane program considering a 16-year lifespan for that program.

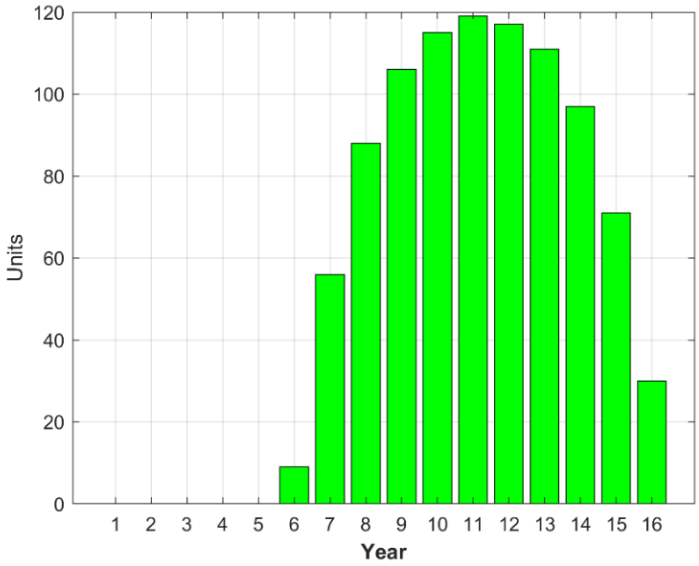

Figure 6 – Example of an aircraft production plan timeline.

3. Case study

3.1 Boeing 757-200

To demonstrate the accuracy of the present methodology for aircraft weight calculation the Boeing 757-200 was chosen for a detailed analysis.

The B757 has a six-abreast cross-section and is powered by either RB211 or PW2030 and PW2040 Series turbofans. The B757-200 is the basic version, which entered service in 1983.

In August 1978, Eastern Airlines and British Airways announced orders for the B757 and choose the RB211-535 to equip the airplane [25]. Designated RB211-535C, the 3-spool engine entered service in January 1983 when the first B757-200 was delivered to Eastern Airlines. The engine has a nominal thrust of 37,400 lb (166.36 kN) and an OPR of 21.2:1 [26]. In 1979, Pratt & Whitney launched its PW2000 engine, claiming 8% better fuel efficiency than the -535C for the PW2037 version [25]. The English engine manufacturer reacted and using the -524 core as a basis, the company developed the 40,100 lb (178 kN) thrust RB211-535E4, which entered service in October 1984. There are differences in appearance between the two versions like a mixed exhaust nozzle and a bigger fan cone for the RB211-535E4. BPR was slightly reduced to 4.40:1 from 4.46 for the 535C [26]. There is another version of the Rolls&Royce engine designated RB-211E4B, which has a takeoff thrust of 43,500 lb [27]. The 535E4 engine was also the first to use the wide chord fan which increased efficiency, reduced noise, and gives increased protection against damage for foreign object ingestion [25]. As a result, a relatively small number of -535Cs were installed on production aircraft. in May 1988, American Airlines ordered 50 B757s powered by the -535E4 emphasizing the engine's low noise as an important factor for its choice. The stretched version B757-300 entered service with Condor Flugdienst in 1999. With a length of 54.5 m, the type is the longest single-aisle twinjet ever built.

According to Ref. [28], The B757-200 has several sub-versions presenting different MTOW, OEW, and MZFW. Two configurations fitted with RB211-535E4B engines were selected as references for the present work, and their payload-range diagrams are shown in Figure 7 and some characteristics are given in Table III [27]. Two ranges signaled by the dashed lines in the payload-range diagrams are related to a mission with a payload of 192 passengers accommodated into two classes.

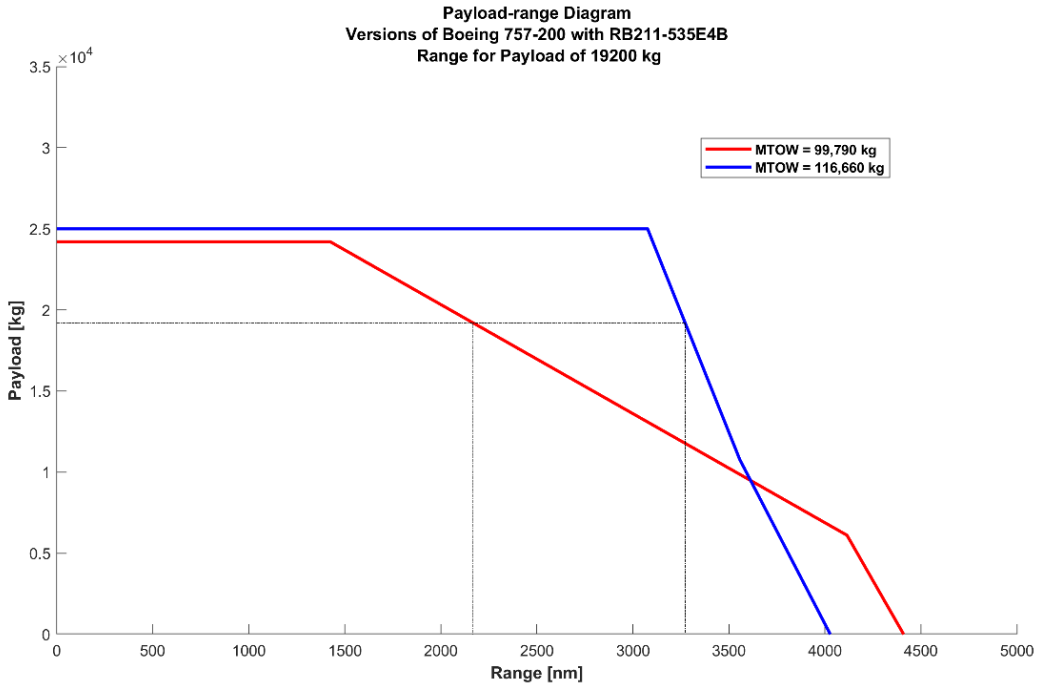

Figure 7 – Payload-range diagram for some sub-versions of B757-200 [27].

Sub-version	MTOW	OEW	MZFW	Usable fuel	Takeoff Thrust	Takeoff field length
1	99,790 kg	59,300 kg	83,460 kg	42,680 kg	2x40,200 lb	1,660 m
2	115,660 kg	59,300 kg	84,360 kg	43,490 kg	2x43,500 lb	2,070 m
Fuselage length	**Aspect ratio**	**Wing area**	**Wing sweep**	**MMO**	**Aisle width of Y-class**	
46.97 m	7.82	185.25 m^2	25º	0.86	0.508 m	

Table III – Characteristics of two B757-200 sub-versions fitted with RB211-535E4B engines [29] [27] [26] [25].

Some of B757-200 main characteristics calculated by the present methodology are given in **Table IV**. The aerodynamics of wing-fuselage-winglet combinations was calculated with an ANN system [30], an improvement relative to Ref. [14]. The remaining aircraft components are calculated by a Class-II approach. The agreement between the characteristics of the actual airplane and its computational representation is exceptionally good.

MTOW	OEW	Fuel Capacity	Range	Engine by-pass ratio	DOC
114,905 kg α	58,452 kg α	41,138 kg β	3,272 nm α	4.40:1	24.41 US$/nm ε
α @ FL370 and FL390, Mach of 0.80, payload of 19,200 kg, ISA+0 ºC, takeoff with MTOW, RB211-535E4, 200 nm to an alternate, 30 min loiter @ 1,500 ft					
β wing capacity of 30,918 kg					
ε Jet A1 price of US$ 2.387 US$/gal, engine weight of 3,500 kg					

Table IV – Estimated values for the B757-200 fitted with RB211-535E4 by the present design framework.

3.2 Aircraft for the Brazilian study

Since this study intends to find out combinations of airplanes of different passenger capacity that are best suited for a set of cities in Brazil presenting passenger demands, an airplane databank was generated following the methodology that was described in the preceding sections. The airplanes that compose the databank feature different engine characteristics and configurations as well as different wing planform and airfoils. Fuselage seating abreast and passenger accommodation are other parameters that make the airplanes different from each other. Finally, field and cruise performance are additional parameters that drove the design of the airplanes. In total, 42 airplanes were generated and some of them are displayed in Figure 8.

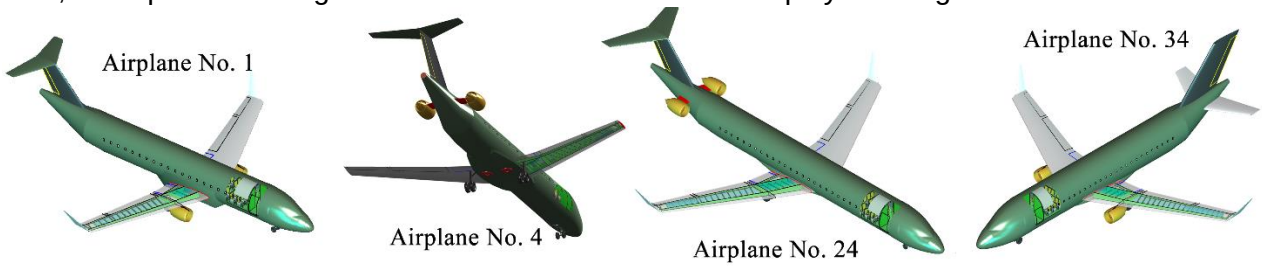

Figure 8 - Some airplanes that compose the database (not on the same scale).

Figure 9 shows two kinds of DOCs: the cost per nautical mile flown (DOC1) and the cost per nautical mile per passenger. The tendency is clear that the larger the wing area, and therefore the passenger capacity, the larger the DOC1 is. DOC2 presents an inverse behavior to that registered for DOC1. Table V contains some characteristics of all airplanes used in the present study.

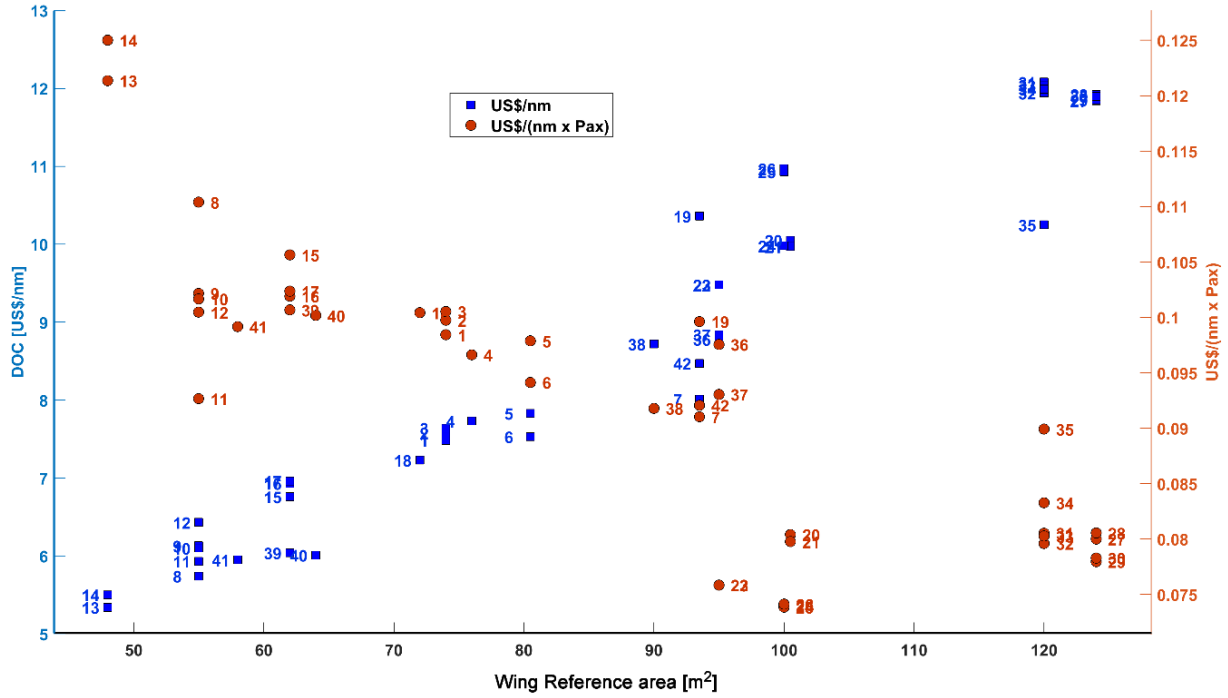

Figure 9 - US$/nm and US$/(nm x Pax) as a function of wing reference area for the airplanes that compose the databank used in the present simulations.

In the present study, the transport network is considered the 21 major airports in Brazil. Distances d_{ij} (used in the network optimization module) and true headings Θ_{ij} (used in the mission analysis module) between city pairs are determined via haversine formula for loxodromic routes [31], according to:

$$a = sin^2\left(\frac{LAT_j - LAT_i}{2}\right) + \cos(LON_i)\,.\,cos\left(LON_j\right).sin^2\left(\frac{LON_j - LON_i}{2}\right) \tag{11}$$

$$c = 2.\arctan\left(\sqrt{\frac{a}{1-a}}\right) \tag{12}$$

$$d_{ij} = R \cdot c \tag{13}$$

$$\theta_{ij} = \arctan\left(\frac{\sin\left(LON_j - LON_i\right).\cos\left(LAT_j\right)}{COS\left(LAT_j\right).SIN\left(LON_j\right) - SIN(LON_i).COS\left(LAT_j\right).COS\left(LON_j - LON_i\right)}\right).\frac{180}{\pi} \tag{14}$$

In **Eq. 13**, R is earth's average radius (6.367 km = 3.438 nm).

A bias of 3% is applied on all great circle distances to accommodate airway-route differences. The airport data used in the mission analysis computations was extracted from the Brazilian Aeronautical Information Publication (AIP) [32]. It is assumed that the airline operating this network has 20% of the passenger market share and does not actuate in the cargo segment. The demand model of **Eq.4** was calibrated using the city pair demands data for the 21 chosen Brazilian routes in 2014, 2015, and 2016, which were obtained from the Brazilian Civil Aviation Authority (ANAC) statistical reports [33]. A log-linear regression model was applied to calibrate the exponents for the proposed equation. Values that were obtained were: K_0=3.5770, K_1=0.4157, K_2=-0.0388, K_3=-0.1643, and K_4=0.1331. The value of 0.63 for the Pearson regression coefficient can be considered reasonable for air transportation analysis.

Table V - Airplane in the design database

Airplane ID	Passenger single class 32" pitch	Seating abreast	MTOW [kg]	Wing area [m^2]	Wing aspect ratio	Range [nm]	Engine BPR	Engine location
1	76	4	34,059	74.0	8.55	1800	5.50	1
2	76	4	34,547	74.0	8.55	1800	5.50	2
3	76	4	35,335	74.0	8.55	2000	5.50	2
4	80	4	36,440	76.0	8.55	2000	5.50	2
5	80	4	38,345	80.5	8.55	2100	5.50	2
6	80	4	37,749	80.5	8.55	2100	6.00	2
7	88	4	40,875	93.5	8.85	2100	6.00	2
8	52	4	25,383	55.0	8.96	1700	6.12	2
9	60	4	27,325	55.0	8.75	1700	6.00	2
10	60	4	26,962	55.0	8.75	1700	6.00	1
11	64	4	26,896	55.0	8.75	1700	6.00	1
12	64	4	29,072	55.0	8.75	1700	6.00	2
13	44	4	22,645	48.0	8.70	1700	5.20	2
14	44	3	23,470	48.0	8.70	1700	5.20	2
15	64	4	29,880	62.0	8.20	1700	5.50	2
16	68	4	30,885	62.0	8.20	1700	5.50	2
17	68	4	30,730	62.0	8.20	1700	5.50	1
18	72	4	32,400	72.0	8.20	1700	5.50	1
19	104	5	43,195	93.5	8.80	1290	3.04	2
20	125	5	49,382	100.5	8.55	1590	5.54	2
21	125	5	48,982	100.5	8.65	1590	6.00	2
22	125	5	47,278	95.0	8.65	1590	6.00	2
23	125	5	47,248	95.0	8.65	1590	6.00	2
24	135	5	50,064	100.0	8.75	1590	6.00	2
25	148	6	55,340	100.0	8.75	1600	6.00	2
26	148	6	56,412	100.0	8.75	1800	6.00	2
27	148	6	62,451	124.0	8.75	2100	5.40	2
28	148	6	63,656	124.0	8.75	2300	5.40	2
29	152	6	63,794	124.0	8.75	2400	5.40	2
30	152	5	63,500	124.0	8.85	2400	5.35	1
31	150	6	63,392	120.0	9.00	2200	5.28	2
32	150	6	61,174	120.0	9.00	2000	5.28	2
33	150	6	61,592	120.0	9.00	2000	5.28	1
34	144	6	61,958	120.0	9.00	2200	5.28	1
35	114	6	52,624	120.0	9.00	2200	5.28	2
36	90	5	43,341	95.0	9.00	2200	5.40	2
37	95	5	44,154	95.0	9.00	2200	5.40	2
38	95	5	43,362	90.0	7.90	2200	5.40	2
39	60	4	27,246	62.0	8.00	1600	5.28	2
40	60	4	27,458	64.0	7.90	1600	5.28	2
41	60	4	27,035	58.0	7.90	1600	5.28	2
42	92	4	42,597	93.5	8.30	2400	5.38	2

Remarks:

- Performance calculations: 100-kg passenger; 200 nm alternate; 45-min holding; cruise Mach number at MMO-0.02.
- Besides planform parameters, airplane wings may differ among them by airfoil composition.
- Engine location =1 means underwing configuration; = 2 placed at rear fuselage

Average delays at each airport are considered by the model proposed by Newell [34] as a function of runway configuration and capacity: for departure delays, which occur on the ground, 10 minutes for airports with two or more active runways (for SBGR, SBGL, and SBBR) and 5 minutes for airports with 1 active runway (for SBCT, SBPA, and SBSV). Arrival delays, associated with terminal holdings and cruise speed reductions, are assumed to be 5 minutes at airports with two or more active runways and 3 minutes for airports with one active runway. Airline operational parameters assumed in this study are listed in **Table VI**. Also, the revenue to ticket price ratio (k_1) and cost to DOC ratio (k_2) is assumed as 1.1 and 1.3, respectively.

Table VI - Airline Operations Parameters.

Parameters	Value
Average Daily Aircraft Utilization [h]	12
Average Turn Around Time [min]	45
Takeoff and Initial Climb out Fuel allowance [kg]	200
Takeoff and Initial Climb out Time allowance [min]	3
Approach and Landing Fuel allowance [kg]	100
Approach and Landing Time allowance [min]	2
Go Around Fuel allowance [kg]	200
Go Around Time allowance [min]	3
Average Taxi Out Time (from gate to runway threshold)	10
Average Taxi In Time (from runway exit to gate)	5
Total Passenger Weight (including baggage)	100
Average Ticket Price [US$]	110 or 200
Average Inflight Delay Cost [US$/min]	20
Fuel Cost [US$/kg]	1.431 or 2.80
Total Operational Costs/Direct Operational Costs ratio	1.3
Total Revenue/Ticket Revenue ratio	1.1

4. Analysis of results for Brazilian network

Brazil represents a significant aviation market in the world with 112.5 million passengers transported in 2017, with 90.6 million in domestic flights, according to ANAC [35]. The revenue of the major airlines reached US$ 11.8 billion considering an average exchange rate of 3.20 Dollar/Real [35]. The optimization tasks carried out here considered 21 Brazilian cities with their passenger demands calculated by a gravitational model.

Some optimization tasks were performed with the baseline one considering an average ticket price of US$ 110 and the fuel price per kg of US$ 1.431. For the second optimization run, the average ticket price was increased to US$ 200. Finally, the third simulation set up the average ticket price back to US$ 110 but increased the fuel price per kg to US$ 2.80. All runs were finished after approximately 55 generations with the genetic algorithm MOGA-II from MATLAB®.

Figure 10 shows the Pareto front that resulted from the baseline optimization run considering the objective functions network daily profit and fleet acquisition amount. For clarity, just some unfeasible individuals are marked by empty circles. Airplane No. 25, a 148-seat 6-abreast airliner

is present in all triplets of the Pareto front. In the low-capacity segment, both 44-seat and 60-seat airplanes were selected. In the middle-capacity sector, there is a larger seat variation, ranging from 72 to 95. Figure 11 shows flight connections performed by airplanes of P1 individuals belonging to the Pareto front. The network with maximum profit (P4), i.e., those operated by airplanes Nos. 10, 18, and 25. As for the P1 solution, Manaus, the capital of that state of Amazon, is not served by any flight. Table VII contains a summary of the Pareto individuals and the network density.

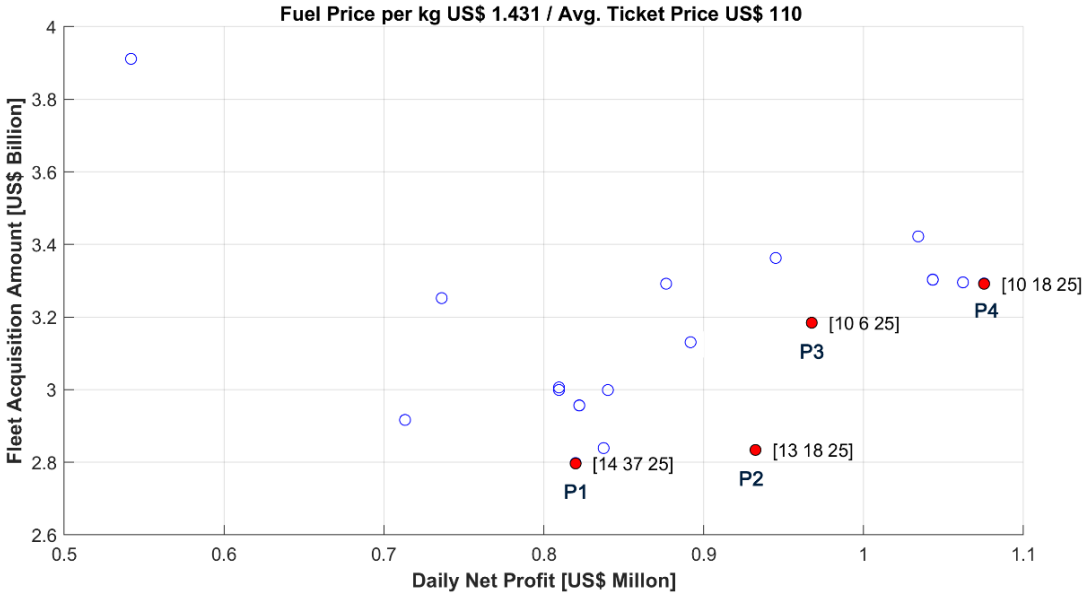

Figure 10 - Pareto front of the baseline optimization task. Some dominated individuals are shown in empty blue circle markers only for clarity (Fuel price/kg = US$ 1.431; Average ticket price = US$ 110).

Table VII - Individuals selected in the Pareto front that resulted from the optimization task.

Design ID	Airplane ID	Seat Capacity	Design Range [nm]	MTOW [kg]	Network Density	List price [in million US$]	Network Profit [in million US$]
P1	AC1	14	44	1,700	23,470	0.29	30.9	0.82
	AC2	37	95	2,200	44,154		69.5	
	AC3	25	148	1,600	55,340		67.6	
P2	AC1	13	44	1,700	22,645	0.32	30.5	0.93
	AC2	18	72	1,700	32,400		49.8	
	AC3	25	148	1,600	55,340		67.6	
P3	AC1	10	60	1,700	26,962	0.30	38.0	0.97
	AC2	6	80	2,100	37,749		57.2	
	AC3	25	148	1,600	55,340		67.6	
P4	AC1	10	60	1,700	26,962	0.31	38.0	1.08
	AC2	18	72	1,700	32,400		49.8	
	AC3	25	148	1,600	55,340		67.6	

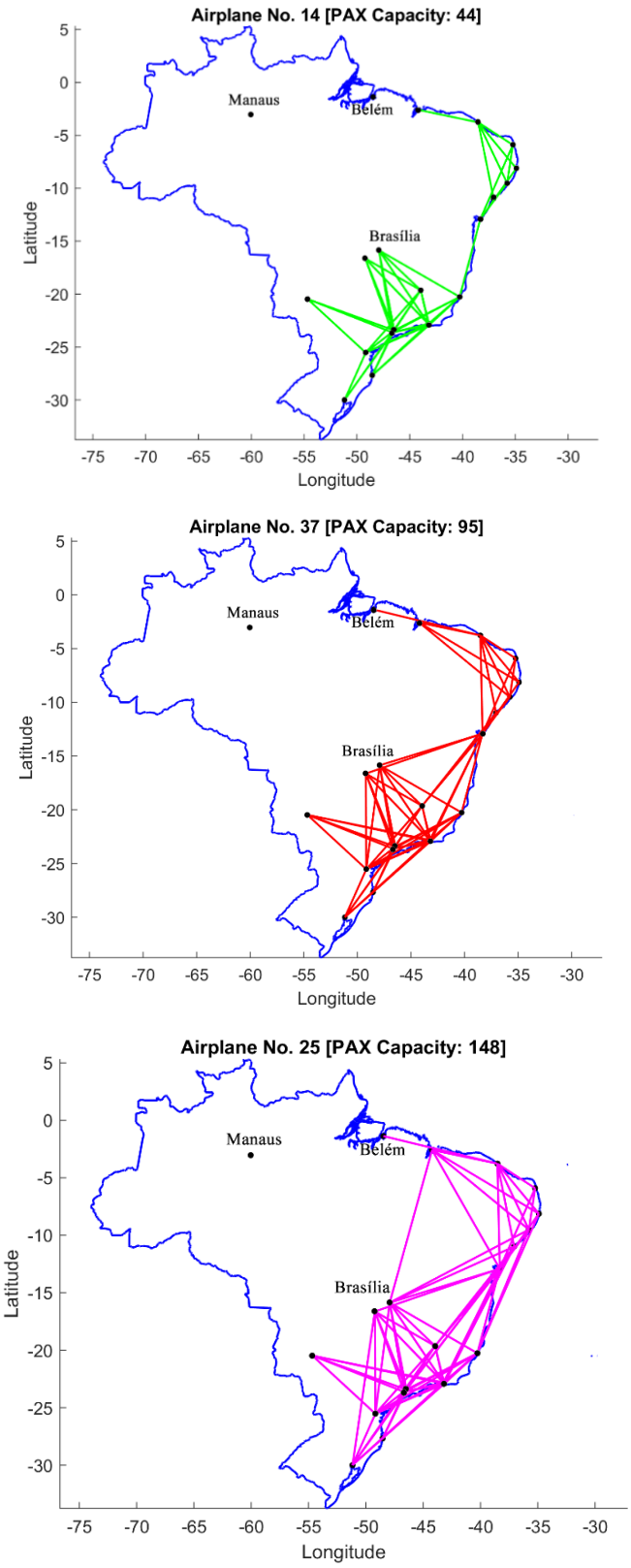

Figure 11 - Network P1 to fulfill Brazilian passenger demands. From top to bottom, routes are performed by Airplanes 14, 37, and 25, respectively.

Table VIII provides details of the four networks belonging to the Pareto front of the baseline optimization run. The amount of money for fleet acquisition ranges from 2.8 to 3.3 billion USD and on average 60 thousand passengers are transported daily. The characteristics of the network with maximum profit rewritten to a yearly basis reveals total passenger transportation of 108.5 million and total revenue of US$ 13.7 billion, which is in good agreement with the data from ANAC [35].

Table VIII - Characteristics of optimal individuals from the baseline optimization.

Parameter	P1	P2	P3	P4
Total Distance flown [nm	394,262	433,761	414,085	422,694
Clustering index	0.60	0.67	0.59	0.63
Passengers boarded	59,556	62,191	60,385	61,871
Estimated CO_2 emission [t]	1928	2013	1938	1978
Fuel [t]	628	638	615	628
Operating cost [US$]	6,386,342	6,592,721	6,339,009	6,410,966
Revenue [US$]	7,206,276	7,525,111	7,306,585	7,486,391
Profit [US$]	819,933	932,390	967,576	1,075,424
Network DOC [US$/nm]	12.5	11,7	11.8	11.7
Profit index [US$/(PAX.nm)]	3.491×10^{-5}	3.46×10^{-5}	3.87×10^{-5}	4.11×10^{-5}
Estimated number of airplanes	50	57	59	64
Fleet purchase amount [US$ Billion]	2.797	2.833	3.184	3.293
Fleet yearly-investment profit ratio	9.345	8.324	9.016	8.389

For another optimization task, the average ticket price was raised to US$ 200. Naturally, this impacts passenger demand, but this was not considered here for simplicity reasons. The resulting Pareto front is shown in Figure 12, revealing a huge increase in operating profit for the individuals in Pareto front. In this scenario, the 60-seat airplane (No. 10) left the scene, which is now dominated by 44-seat airplanes (twinjets No. 13 and 14). In the capacity range above 99 seats, airplane No. 25 was joined by the 135-seat airplane No. 24 and the slightly heavier airplane No. 26. The triplet P7 seems to be a natural choice to this Pareto front that emerged because profit is outstanding with a slight increase of the fleet purchase cost when compared to the P2 to P6 individuals.

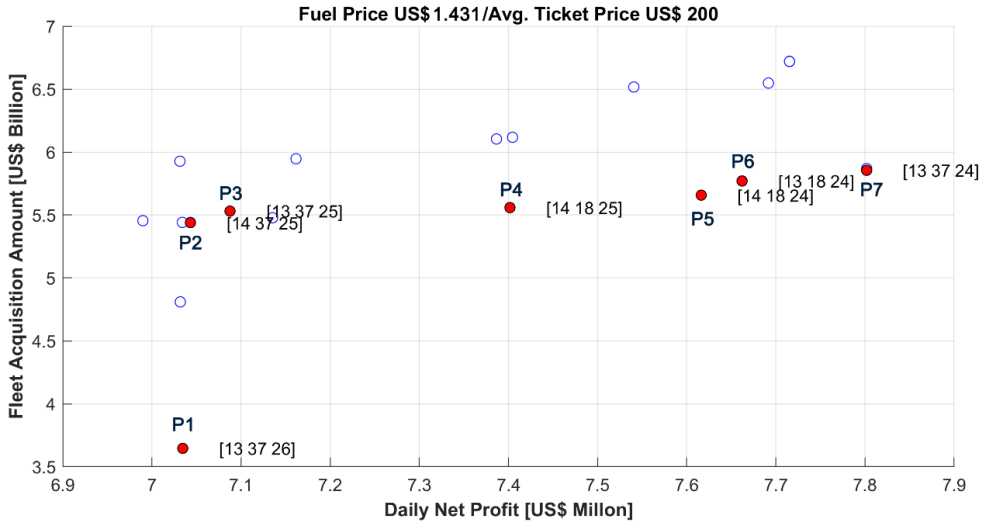

Figure 12 - Pareto front of the optimization task with the increased average ticket price. Some dominated individuals are shown in empty blue circle markers only for clarity.

Figure 13 shows the airplane connections operated by the triplet {13, 37, 24} airplanes for the simulation with the increased average ticket price. The increase in the number of connections among cities regarding the previous simulation is noticeable. Manaus is now served by air service, by airplanes Nos. 37 and 24. Table IX shows relevant data related to the P7 network, which records a daily profit of US$ 7.8 million.

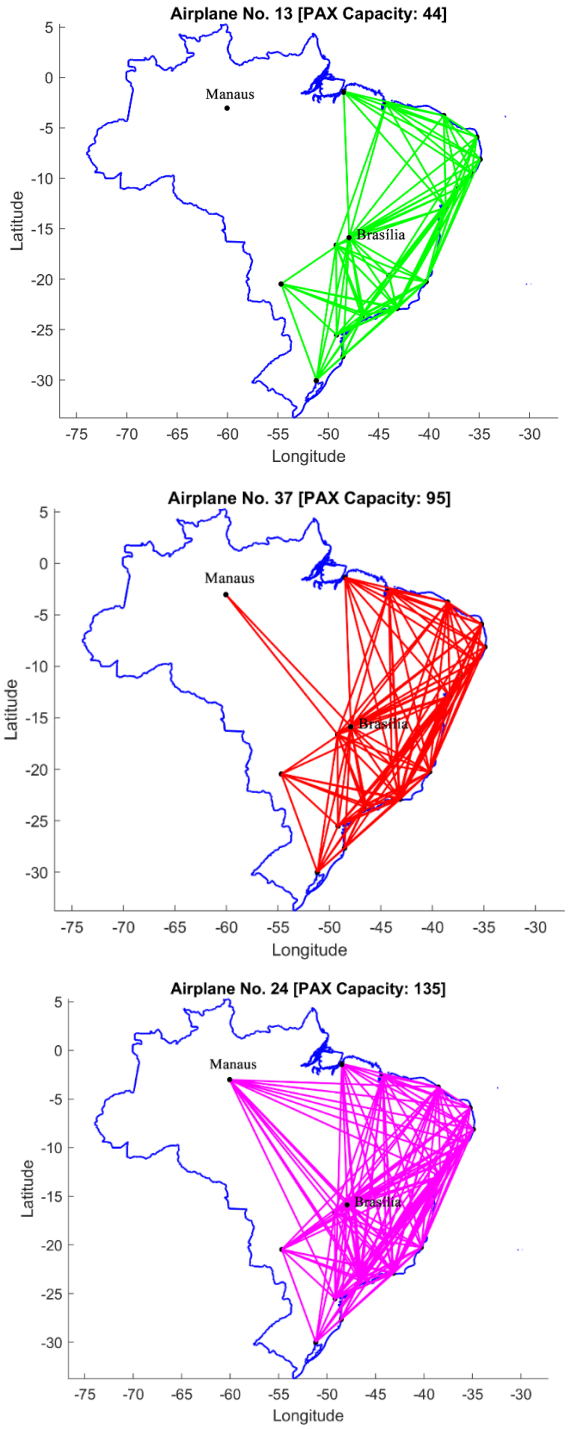

Figure 13 - The individual P7 from the Pareto front of the second simulation (increased ticket price).

Table IX - Data for the network with maximum profit (P7).

Parameter	Value
Total Distance flown [nm]	1,426,771
Avg. network clustering index	0.66
Number of passengers	126,577
Estimated CO_2 [ton]	1928
Total fuel [ton]	1873
TOTAL COST [US$]	20,045,005
TOTAL REVENUE [US$]	27,846,940
TOTAL PROFIT [US$]	7,801,934
Network DOC [US$/nm]	10.8
Network Profit [US$/PAX. nm].$10^{-5}$	4.32
Estimated number of aircraft	112
Airline's Total Fleet Investment [Billions of US$]	5.853
Fleet investment-yearly profit ratio	2.06

A simulation with increased fuel price was run and the resulting Pareto front is shown in Figure 14 The aircraft combination {14,18,25} is the single individual from Pareto presenting a profit. This is an individual already present in fronts from previous optimization runs and Table X contains some relevant data for its network. Figure 15 shows only a few connections, with the daily profit now approximately US$ 50,000.

Table X - Individual characteristics for the network with increased fuel price

Parameter	Value
Total Distance flown [nm]	227,601
Number of passengers	43,375
Estimated CO_2 [ton]	1140
Total fuel [ton]	362
TOTAL COST [US$]	5,202,220
TOTAL REVENUE [US$]	5,248,375
TOTAL PROFIT [US$]	46,155
Network DOC [US$/nm]	17.6
Network Profit [US$/PAX. nm].$10^{-5}$	4.68
Estimated number of aircraft	28
Airline's Total Fleet Investment [Billions of US$]	1.380
Avg. network clustering index	0.56

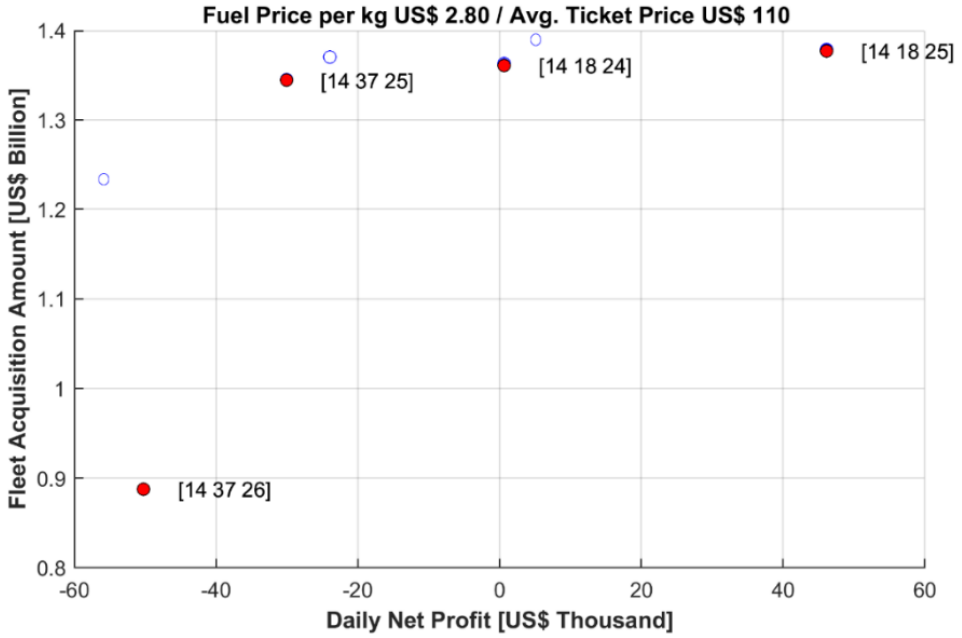

Figure 14 - Pareto front of the simulation with increased fuel price.

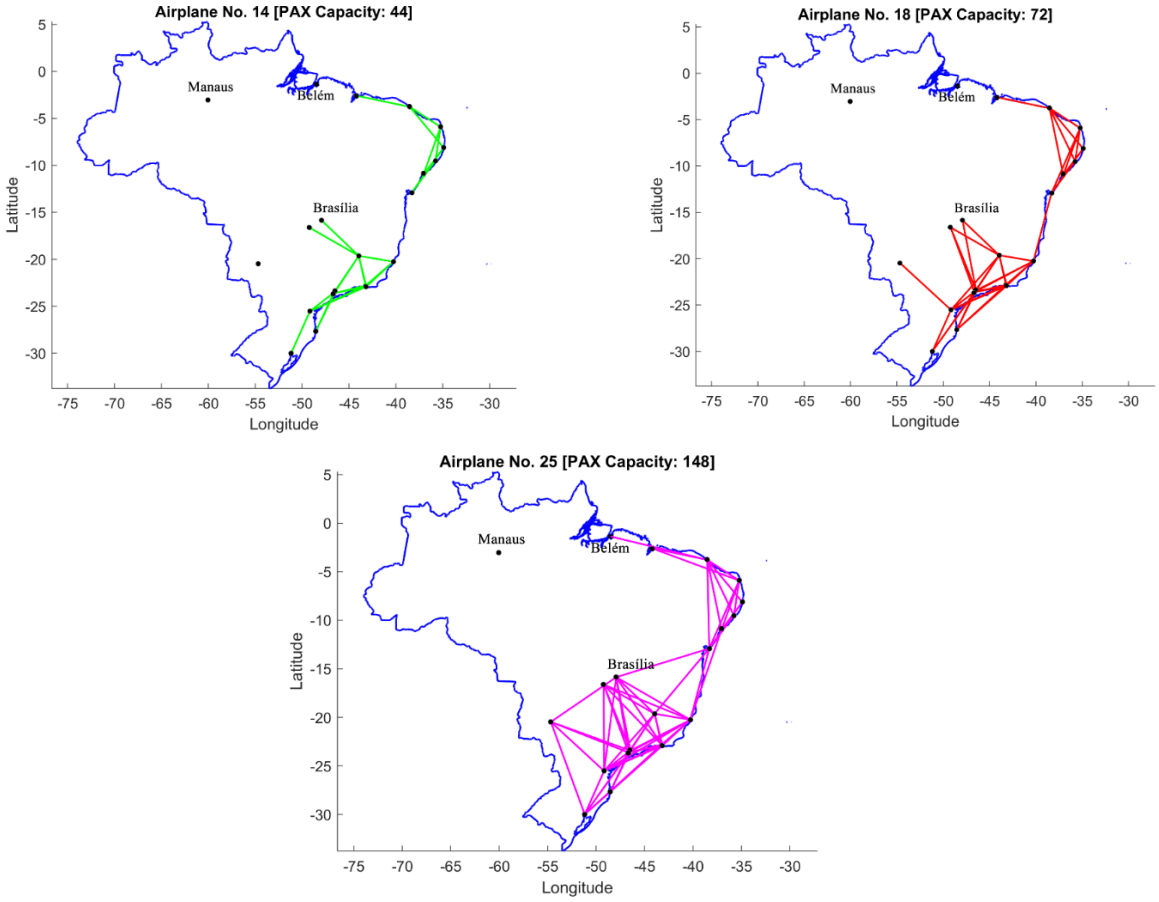

Figure 15 - Connections displayed are performed by Airplanes No. 14, 38, and 25 from the simulation that considered increased fuel price.

5. Further improvements in aircraft performance and economics

All 42 aircraft utilized in the Brazilian network (**Table V**) have the same basic wing airfoils. These airfoils are typical transonic geometries, which poses a certain limitation of the present analysis.

Aircraft can be improved and inserted into the database for evaluation of its performance in airline networks. Improvements may come from optimizations of aircraft geometry and topology or even from the introduction of technologies such as laminar flow, lighter structures, and so on. This is one of the advantages of the present methodology.

To illustrate this approach, an aerodynamic optimization of an airplane similar in capacity to the B757-200, which is described in Section 3.1, was carried out. The airplane is designated here BF-200LR and its top view is compared to that of B757-200 in Figure 16. Basic data for BF-200LR is given in Table XI.

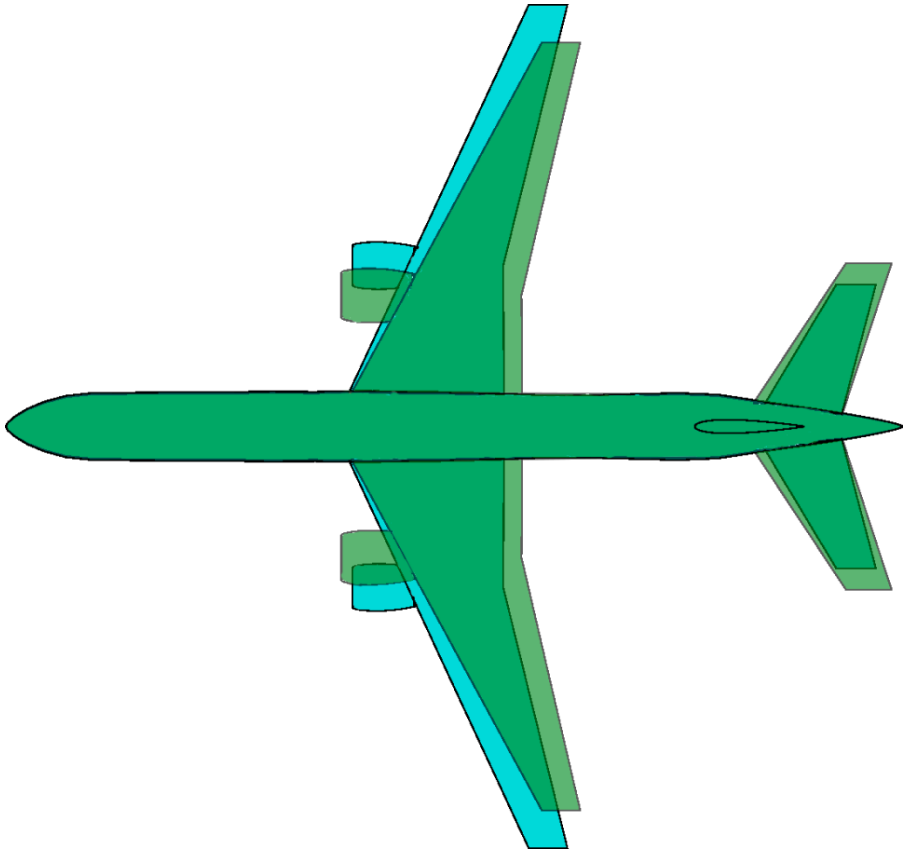

Figure 16 - B757-200 and BF-200LR top-view juxtaposition for comparison purposes.

Table XI – Basic data for BF-200LR.

Wing Aspect ratio	**Wing area**	**Wing sweep**	**Overall thrust**	**Engine BPR**	**Engine diameter**	**Two-class accommodation**	**Design range**
9.97	175.35 m^2	22.29º	285.6 kN	6.00:1	1.93 m	192	3,420 nm
MTOW		**OEW**		**MMO**	**Fuel capacity**		**Range**
100,111 kg		53,573 kg		0.81	30,924 kg		3,470 nmα
α @ FL370 and FL390, Mach number of 0.80, payload of 19,200 kg, ISA+0 ºC, takeoff with MTOW, 200 nm to an alternate, 30 min loiter @ 1,500 ft							

This additional study was intended to design the break- and tip-station airfoils, jointly to find out the optimal wing twist angle, and the incidence of the break station for a set of objectives and constraints.

Airfoil geometry impacts enormously the maximum lift coefficient. According to Ref. [36], the C_{Lmax} at landing for the B757-200 is 2.38, considerably lower than that of its computational representation airplane considered here, which presents a value of 3.06 for this coefficient. This is due to the different wing airfoil geometries that compose the actual airplane and its counterpart of the present work. There is no information available about the B757-200 airfoils and that utilized here are transonic airfoils that intend to match the maximum relative thickness of them as close as possible. On the other hand, the MMO of B757-200 is 0.86 [36], relatively high considering the moderate sweepback angle of its wing. Despite the typical mission established for the B757 was to fly domestic routes in the United States, even for medium populated cities, the North American manufacturer preferred a configuration with higher speed, which certainly had an impact on field performance.

In general, airfoils presenting good transonic characteristics like higher divergence Mach number tend to reveal some degradation of field performance. Thus, an optimization with these two conflicting objectives may produce interesting results.

The optimization task that was then carried out included two objectives:

- the maximum value of the Mach x Lift/Drag (MLD) in the 0.70 -0.85 Mach number range,
- and the maximum lift coefficient at landing configuration.

The constraints for this problem are:

- the maximum relative thickness of break-station airfoil greater than that of tip-station airfoil.
- The maximum relative thickness of root-station airfoil greater than that of the break-station airfoil.
- MMO must be higher than 0.80.
- Fuel capacity greater than 30,000 kg.
- C_{Lmax} must be higher than 2.5.

The aerodynamic coefficients at the transonic regime for this simulation were calculated by an ANN system with 64 input variables for wing-fuselage-winglet combinations [30] and the remaining aircraft components a Class-II approach was employed. The airfoils were generated by 14 weights applied to the geometry of 14 airfoil geometries composing a database. Thus, 42 input variables are necessary to define the geometry of three basic wing stations, root, break, and tip. The clean-wing maximum lift coefficient is calculated by a full-potential code in combination with a 2D panel code by the critical section method. Utilizing this information and additional configuration characteristics, the Datcom method is then employed for the estimation of the C_{Lmax} coefficients at landing and takeoff configurations.

The simulation for airfoil optimization was stooped after 20 generations with 1200 individuals being analyzed. Figure 16 shows the Pareto front and the characteristics of feasible and unfeasible individuals that arose in the simulation. A considerable improvement of MLD for the reference airplane was obtained, the same cannot be said for the C_{Lmax}. Figure 17 compares the original and optimized airfoils that resulted from the optimization run.

Table XII shows the characteristics of a selected individual from the Pareto front. MMO of 0.82 was obtained with the utilization of the surrogate ANN system considering a lift coefficient of 0.50. The aircraft module of the present design framework calculated the MTOW based on the same mission as that for the BF-200LR of maximum takeoff thrust, and a value of 97,841 kg was obtained. This is considerably lower than that shown in Table XI, of our reference airplane. However, this be only credited to the new airfoils, because MMO was increased from 0.81 to 0.82. A lower MMO means lower structural loads, and this will lead to a lower OEW. In addition, an aircraft with a similar mission of B757-200 when fitted with new, high by-pass engines, higher aspect ratio wings, and optimized airfoils, recorded a 17-t decrease in MTOW.

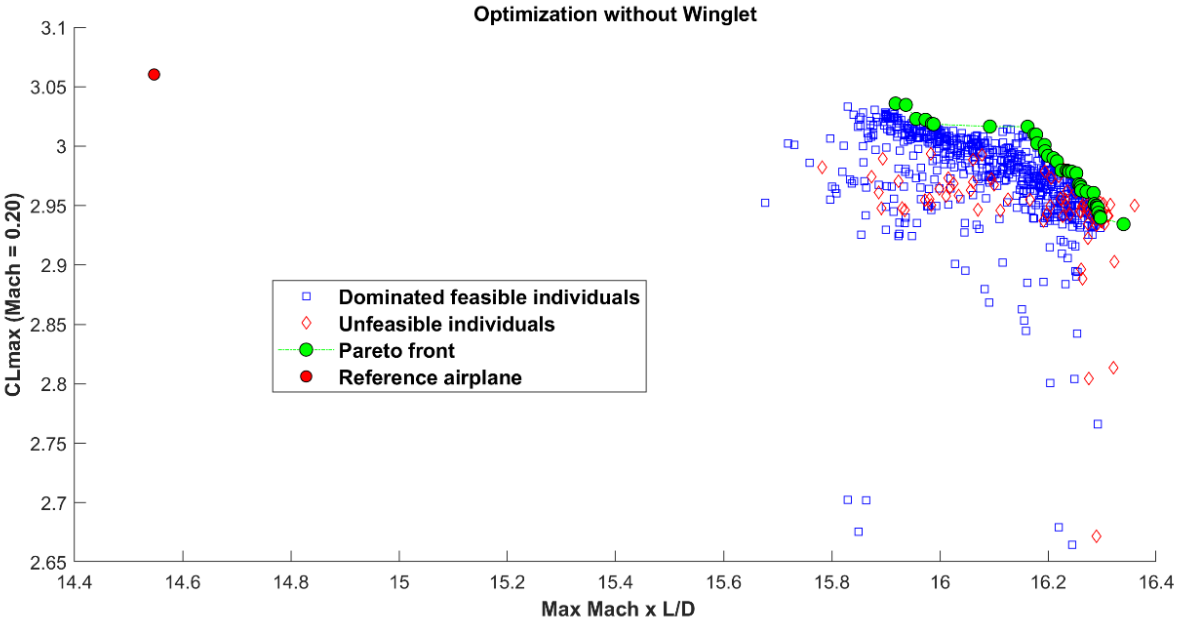

Figure 16 – Optimization of wing airfoil geometry for a B757-200 similar aircraft.

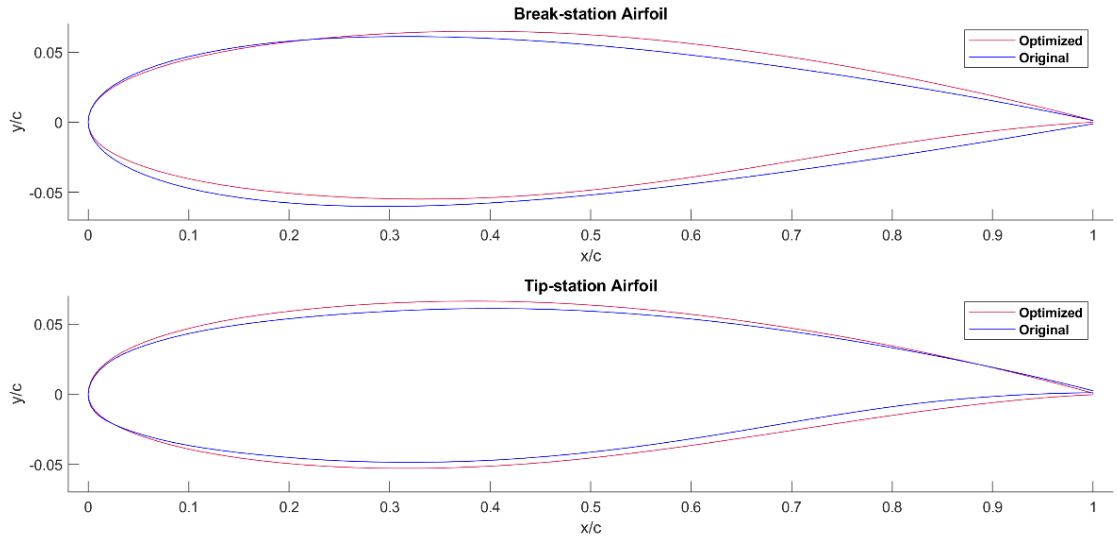

Figure 17 -Break- and tip-station airfoils of the selected airplane optimal configuration.

Table XII – Optimization of wing airfoils of BF-200LR.

Parameter	Value
Max. MLD	16.21
C_{Lmax} landing configuration (Flap 40º)	2.987
C_{Lmax} clean wing	1.59
MMO	0.82
Fuel capacity	31,287 kg
Max. relative thickness of root airfoil	15.1%
Max. relative thickness of the break-station airfoil	12.0%
Max. relative thickness of tip airfoil	11,9%
Wing twist angle	-3.74º
Incidence of wing break station	0.276º
OEW	52,854 kg
ΔMTOW$^{\alpha}$	-2,270 kg

α @ FL370 and FL390, Range of 3,470 nm @ Mach number of 0.80, payload of 19,200 kg, ISA+0 ºC, takeoff at MTOW, 200 nm to an alternate, 30 min loiter @ 1,500 ft

6. Conclusions

The integrated transportation system design approach of the present work enables a detailed analysis of the two different main components, namely the airplane and city connections, that comprise the transportation system and define how they work together. Utilizing the formulations developed to define the network, airplanes, and cities to be served by air transport, a concurrent optimization of the transportation system can be obtained. The methodology was applied to a Brazilian network consisting of 21 major airports in that country. The demand for those cities was generated by using a gravitational model. In addition, a database consisting of 42 realistic and detailed airplanes with different seating capacities was generated. Accurate calculation of true mission profiles was performed, thanks to an ANN model for aerodynamic coefficient estimation, a robust generic turbofan engine deck, and another proper modeling of aeronautical disciplines.

Three optimization runs were carried out considering variations of the average ticket and fuel prices. The highlighted airplanes, which are present in the three optimization runs and recorded better profit, are the No. 14, 18, 24, and 25, a 44-seater, a 72-passenger twinjet, a 135-seater 5-abreast jetliner, and a 148-seater 6-abreast airliner, respectively. Considering the baseline scenario, the 60-seat No. 10 is a good choice. The 148-seat No. 25 is undoubtedly a forerunner, able to guarantee a minimal profit, in combination with the Nos. 14 and 18 in times of rising fuel prices. It is comparable in terms of passenger capacity with Airbus A220-300 and the veteran McDonnell Douglas MD-87.

The impact of the introduction of turboprop into the airplane database is something important to analyze in the future. They may eventually replace the 44-seat twinjets that emerged in some optimal solutions. Among the three largest airlines that operate domestic flights in Brazil, Azul Airlines is the only one that operates a combined fleet of jet and turboprop airliners.

With the inclusion of the vehicle and network into the transportation system operations, a more efficient network architecture can be obtained that reduces operating costs or maximizes profit. This methodology can be applied to strategic planning or investments at a major cargo or passenger airline or provide insight about market needs to aircraft designers. The present methodology can also be used to evaluate, for example, the impact of consideration of scope clause issues or airplane emissions on network topology.

7. Contact author e-mail address

José Fregnani: fregnani@ita.br

8. Copyright statement

References

[1] R. Doganis, Flying Off Course IV: Airline Economics and Marketing, Routledge, DOI: 10.4324/9781315402987, 2009.

[2] J. C. Medau, *Allocation of aircraft to flights considering aircraft operational, maintenance and performance restrictions*, São Paulo: University of São Paulo, 2017. Available: https://teses.usp.br/teses/disponiveis/3/3138/tde-25082011-134443/pt-br.php.

[3] D. Klabian, Large-scale models in the airline industry, Kluwer Academic Publishers, DOI: https://doi.org/10.1007/0-387-25486-2_6, 2014.

[4] A. Rabetanety, J. Calmet and C. Schoen, *Airline Schedule Planning Integrated Flight SChedule Design and Product Line Design*, Karlsruhe: University of Karlsruhe, DOI:https://doi.org/10.1287/trsc.1030.0026, 2006.

[5] C. Hane, C. Barnhart, C. Johnson, E. Marsten, R. Nemhauser, and G. Sigismondi, "The fleet assignment problem: solving a large-scale integer program," Georgia Institute of Technology, DOI: http://doi.org/10.1007/BF01585938, 1995.

[6] B. S. Mattos, J. A. Fregnani and P. C. Magalhães, Conceptual Design of Green Transport Airplane., Book Series: Frontiers in Aerospace Science ed., vol. 3, Bentham Books, DOI: http://doi.org/10.2174/97816810832781180301, 2018.

[7] J. A. Reed, G. Fallen, and A. A. Afjeh, "Improving the Aircraft Design Process Using Web-based Modeling and Simulation," NASA Glenn Research Center, Hanover, MD, 2000. Available: https://pdfs.semanticscholar.org/7fd7/db15a53c7c7720fa68b55b4a1f64a63f04ba.pdf.

[8] V. B. Camarotti, “Estudo de Drivers de Mercado, Metodologia e Desenvolvimento de Ferramenta Semi-Automática para Elaboração de Projeções de Mercado de Aviação de Linha,” undergraduate thesis, Instituto Tecnológico de Aeronáutica, São José dos Campos, 2014. Availble: http://www.bibl.ita.br/.

[9] C. Taylor and O. de Weck, "Integrated Transportation Network Design Optimization," in *47th AIAA/ASME/ASCE/ASC Structural Dynamics, and Materials Conference*, Newport, 2006. DOI: https://doi.org/10.2514/6.2006-1912.

[10] J. Fregnani, B. S. Mattos and J. A. Hernandes, "An Innovative Approach for integrated Airline Network and Aircraft Family Optimization," in *AIAA Aviation Forum 2019*, Dallas, DOI: https://doi.org/10.2514/6.2019-2865, 2019.

[11] Mathworks Inc., "Mixed-Integer Linear Programming Algorithms," Mathworks Inc., September 2019. [Online]. Available: https://www.mathworks.com/help/optim/ug/mixed-integer-linear-programming-algorithms.html#bt6n8vs. [Accessed September 2019].

[12] N. R. Secco and B. S. Mattos, "Artificial Neural Networks Applied to Airplane Design," in *53rd AIAA Aerospace Sciences Meeting, AIAA SciTech Forum*, 2015, DOI: http://dx.doi.org/10.2514/6.2015-1013.

[13] M. Drela and H. Youngren, "AVL Overview," Massachusetts Institute of Technology, December 2019. [Online]. Available: http://web.mit.edu/drela/Public/web/avl/. [Accessed December 2019].

[14] B. S. Mattos, and N. R. Secco, "An Airplane Calculator Featuring A High-Fidelity Methodology for Tail Sizing," *Journal of Aerospace Technology and Management*, pp. 371-386, 2013, DOI: http://dx.doi.org/10.5028/jatm.v5i4.254.

[15] Y. Zang, "Solving Large-Scale Linear Programs by Interior-Point Methods under MATLAB environment," Baltimore, 1995, DOI: http://doi.org/10.1080/10556789808805699.

[16] C. M. Fonseca and P. J. Fleming, "Genetic Algorithms for Multiobjective Optimization: Formulation, Discussion, and Generalization," in *Proceedings of the Fith International Conference*, San Mateo (CA), 1993.

[17] E. Torenbeek, Advanced Aircraft Design, Wiley & Sons, 2013, DOI: 10.1002/9781118568101.

[18] A. K. Kundu, Aircraft Design, Cambridge University Press, 2010, DOI: http://doi.org/10.1017/CBO9780511844652.

[19] P. Langenegger, “Otimização Aero-Estrutural na Fase de Projeto de Aeronave,” Instituto Tecnológico de Aeronáutica, Undergraduation Thesis, São José dos Campos, 2012. Available: http://www.bibl.ita.br/.

[20] P. Jaillet, G. Song and G. Yu, "Airline Network Design and Hub Allocation Problems," *Location Science*, vol. 4, pp. 195-212, 1996, DOI: http://doi.org/10.1016/S0966-8349(96)00016-2.

[21] O. Wojan, "Airline Network Structure and the Gravity Model," the University of Hamburg and Lufthansa Technik AG, Hamburg, 2000, DOI: http://doi.org/10.1016/S1366-5545(00)00026-0.

[22] L. P. Siqueira, V. Loureiro, and S. B. Mattos, "The Suited Airliner for an Existing Airline Network," in *50th AIAA/ASME/ASCE/AHS/ASC Structures, Structural Dynamics, and Materials Conference*, Palm Springs, 2009, DOI: http://doi.org/10.2514/6.2009-2206.

[23] NASA Glenn Research Center, "EngineSim Version 1.8a," NASA, 2018. [Online]. Available: https://www.grc.nasa.gov/WWW/K-12/airplane/ngnsim.html. [Accessed 2018].

[24] J. Morrison, J. Hasman and S. Sgouridis, "Game Theory Analysis of The Impact of Single Aisle Aircraft Competition Fleet Emissions," Massachusetts Institute of Technology, Cambridge, 2011, DOI: http:// doi.org/10.2514/6.2011-6844.

[25] Wikipedia, The Free Encyclopedia, "Rolls-Royce RB211," Wikipedia, The Free Encyclopedia, 2021. [Online]. Available: https://en.wikipedia.org/wiki/Rolls-Royce_RB211. [Accessed May 2021].

[26] European Union Aviation Safety Agency, "Type-Certificate Data Sheet for Rolls&Royce for RB211-535 Series Engine," EASA, Cologne, 2020.

[27] Boeing Commercial Airplanes, "Boeing Resources," 2021. [Online]. Available: https://www.boeing.com/resources/boeingdotcom/company/about_bca/startup/pdf/historical/757_passenger.pdf. [Accessed May 2021].

[28] Boeing Commercial Airplanes, "Boeing 757 Airplane Characteristics for Airport Planning," Boeing, Seattle, 2002.

[29] Boeing Commercial, "777-200/300 Airplane Characteristics for Airport Planning," Boeing Co., Seattle, 1998.

[30] M. Gumes e L. D. Andrade Pereira, "Utilização de Redes Neurais para Estimação de Coeficienets Aerodinâmicos e Derivadas de Estabilidade," Undegraduation thesis, Instituto tecnológico de Aeronáutica,, São José dos Campos, 2019.

[31] C. C. Robusto, "The cosine-harvesine formula," *The American Mathematical Monthly*, pp. 30-40, 1957. Available: https://www.jstor.org/stable/2309088?seq=1.

[32] Brazilian Airspace Control Department, "Aeronautical Information Publication (AIP) - AGA Part," Institute of Aeronautical Cartography, Rio de Janeiro, 2016. Available: htpps://aisweb.decea.gov.br.

[33] Ágência Nacional de aviação Civil, "Anuário do Transporte aéreo 2014, 2015 e 2016," ANAC, Brasília, DF, 2017. Available: https://www.anac.gov.br/assuntos/dados-e-estatisticas/mercado-de-transporte-aereo/anuario-do-transporte-aereo/dados-do-anuario-do-transporte-aereo.

[34] G. F. Newell, "Airport Capacity and Delays," *Transportation Sciences*, pp. 201-241, 1979, DOI: http://doi.org/10.1287/trsc.13.3.201.

[35] Agência Brasileira de Aviação Civil, "Anuário de Transporte Aéreo 2017," ANAC, Brasília, 2018. Available: https://www.anac.gov.br/assuntos/dados-e-estatisticas/mercado-do-transporte-aereo/ultimas-publicacoes/anuario-do-transporte-aereo-2013-2017/view.

[36] L. Jenkinson, P. Simpkin, and D. Rhodes, "Civil Jet Aircraft design - Boeing Aircraft," Butterworth-Heinemann, 2001. [Online]. Available: https://booksite.elsevier.com/9780340741528/appendices/data-a/table-3/table.htm. [Accessed June 2021].